DEVELOPMENT OF IMMUNOMODULATORY, COMPLIANT DECELLULARIZED EXTRACELLULAR MATRICES VIA ALIPHATIC CHAIN MODIFICATION FOR BLADDER TISSUE ENGINEERING

by

Sarah Rajani

A thesis submitted to Johns Hopkins University in conformity with the requirements for the degree of Master of Science in Engineering

Baltimore, Maryland

May 2020

Abstract

Decellularized extracellular matrices (dECMs) are considered ideal scaffolds for tissue regeneration due to their inherent bioactivity. Despite this advantage, the use of dECMs for bladder tissue reconstruction has resulted in inconsistent preclinical model results, including complications such as infection, stone formation, and loss in bladder capacity. These results have been attributed to a mismatch in material properties and the mechanical requirements of the bladder; most notable is the ability to undergo large expansion under minimally applied force.

Here, we present the first study to improve dECM compliance through chemical modification, in order to meet the mechanical functional requirements of the bladder. Aliphatic chains (C18) were incorporated onto porcine small intestinal submucosa (SIS), porcine urinary bladder matrix (UBM), bovine pericardium, bovine dermis, and human dermis scaffolds. The effect of hydrophobe addition on scaffold physical properties, cytotoxicity and immune response was studied. Modified materials exhibited compliance that was comparable to rabbit bladder tissue. Material toughness, evaluated through uniaxial tensile testing, and resistance to enzymatic degradation, specifically collagenase I, increased with minimal change in the swelling profile at 37^{o}C. Direct contact angle measurements were used to investigate surface hydrophobicity and this was found to increase with C18 addition for all dECMs. Human bladder epithelial cells seeded directly on dECMs preferentially adhered to moderately hydrophobic surfaces compared to human bladder fibroblasts and THP-1 macrophages. Modified dECM scaffolds also exhibited improved immunomodulatory capacity, with upregulation of TGFβ and CD163 and downregulation of TNFα and CD86 in macrophages, evaluated *in vitro* using RT-qPCR.

Cell infiltration to the biomaterial center and biomaterial degradation *in vivo,* observed in subcutaneously implanted dECMs, were delayed upon C18 modification at Day 7 but did not show signs of causing graft rejection by Day 21.

Of all dECMs tested, modified bovine pericardium demonstrated the largest improvement in material compliance, the capacity to support cell adhesion, and the greatest shift in macrophage behavior towards a pro-regenerative M2 phenotype. The enhanced compliance of modified materials and favourable immune response suggest that C18-modified dECMs are suitable biomaterials for urologic tissue regeneration.

Primary Reader and Advisor: Dr. Anirudha Singh

Secondary Readers: Dr. Jamie Spangler, Dr. David Gracias

Preface

All experiments presented in this thesis were designed by the author. Data presented here were also collected, analyzed and formatted by the author, with the exception of animal procedures which were performed by a fellow lab member, Shivang Sharma.

This thesis will also be published in the future as a scientific paper.

Rajani S, Sharma S, Hui J, Singh A. Development of immunomodulatory, compliant decellularized extracellular matrices via aliphatic chain modification for bladder tissue engineering. *In preparation*

Acknowledgements

First, I would like to thank Dr. Anirudha Singh for providing me the opportunity to conduct independent research and develop my own skills, both technical and transferrable, over the last year. I would also like to thank Shivang Sharma for his assistance in conducting the animal studies in order to complete a thorough study in biomaterial design and Justin Hui for his support during the research process. I would also like to thank Bryan Wehrenberg for his advice and support this past year. It has been a pleasure and I will always appreciate the learning experience. Finally, I would like to thank my family and friends for their support and encouragement during this time and in the exciting times to come.

Table of Contents

ABSTRACT **II**

PREFACE **IV**

ACKNOWLEDGEMENTS **V**

LIST OF TABLES **VIII**

LIST OF FIGURES **IX**

1 Introduction **1**

2 Experimental Methods **5**

2.1 dECM Scaffold Source 5

2.2 dECM Scaffold Modification 5

2.3 Mechanical Testing 6

2.4 Swelling Ratio, Enzymatic Degradation and Contact Angle Measurements 6

2.5 Human Bladder Epithelial Cell and Fibroblast Proliferation 7

2.6 Immunomodulation *in vitro* 8

2.6.1 Monocyte to macrophage differentiation 8

2.6.2 Macrophage Polarization 9

2.6.3 Gene Expression by RT-qPCR 9

2.7 Biocompatibility *in vivo* 11

2.7.1 Subcutaneous implantation 11

2.7.2 Histological and Immunostaining 11

2.8 Statistical analysis 12

3 Results **13**

3.1 Mechanical Testing 13

3.2 Swelling and Enzymatic Stability 19

3.3 Surface Hydrophobicity and Direct Cell Adhesion 22

3.4 Immunomodulation *in vitro* 25

3.5 Biocompatibility *in vivo* 29

4 Discussion **38**

5 Conclusions **46**

6 References **47**

CURRICULUM VITAE **50**

List of Tables

Table 1. Summary Values from uniaxial tensile testing 16

List of Figures

Figure 1. Uniaxial tensile strength of control and modified dECM 18

Figure 2. Evaluation of swelling behavior and resistance to enzymatic degradation with and without aliphatic chain modification 21

Figure 3. Hydrophobicity and cytotoxicity *in vitro* 24

Figure 4. Surface Marker expression of biochemically polarized macrophages 26

Figure 5. Macrophage polarization *in vitro* 29

Figure 6. *In vivo* subcutaneous biocompatibility of C18-modified dECM scaffolds through cell-material interactions 36

Figure 7. *In vivo* subcutaneous biocompatibility of C18-modified dECM scaffolds through collagen deposition 37

1 Introduction

Bladder dysfunction caused by impaired bladder tissue frequently calls for reconstructive surgeries to prevent injury to the kidneys and the build-up of toxins in the blood[1]. The most common procedure, bladder augmentation using gastrointestinal segments, often results in complications including bacterial infection, stone formation and inflammation[1–3]. It is speculated that these issues are caused by differences in the tissue structure and function of the native bladder tissue and repurposed gastrointestinal segments. Alternative tissue engineering strategies for reconstructive urology have evolved over the last several decades, including the use of different biomaterials, acellular and cell-laden scaffolds, with varying levels of clinical success[4–7]. Thus, there is still a need for the development of a biomaterial suitable for bladder tissue regeneration.

The primary function of the bladder must be considered to guide biomaterial design; the biomaterial, and eventually the newly formed bladder tissue, must be able to support liquid storage, maintain the blood-urine barrier, and withstand cyclic loading and unloading[1,4,8]. In addition to having compatible mechanical properties, the ideal scaffold for regenerative medicine supports cell-matrix interactions for tissue regrowth and modulates the host immune system to give rise to a pro-regenerative environment[5]. Increased understanding of the immune response has shifted design criteria towards promoting interactions between the material and the immune system that elicit a desired response, rather than aiming for the development of an "inert" material. The interactions between scaffolds and cells of the innate immune system, namely dendritic cells, eosinophils, macrophages and NK cells, have been studied to assess the foreign body response *in vitro* and *in vivo* because of their roles in early wound healing and

influence on the adaptive immune cell phenotype[9–11]. Macrophages are of special interest in tissue engineering because of their plasticity; in response to external stimuli, such as a newly implanted biomaterial, these cells differentiate into functional states that exist along a spectrum ranging from a pro-inflammatory or classically activated phenotype ("M1") to a pro-regenerative or alternatively activated ("M2") phenotype[12]. This phenotypic response alters the surface marker expression and cytokine production that influences the response of other innate immune cells, other tissue resident cells, as well as adaptive immune cells, namely T-cells and B-cells. Therefore, macrophages are frequently used to study the effects of material stiffness, microarchitecture and surface chemistry on their differentiation as an indicator of the host immune response[13–15].

Scaffolds derived from decellularized extracellular matrix (dECM) have been extensively studied as viable scaffolds for tissue regeneration. Bioactive molecules, such as growth factors and proteoglycans, naturally present in live tissue survive the decellularization process and serve to induce tissue regrowth, making dECM a particularly attractive biomaterial scaffold for regenerative medicine[4,16]. A variety of sources have been used and approved by the FDA for urologic surgeries including small intestinal submucosa (SIS), pericardium, and urinary bladder matrix (UBM); however, these materials are not approved for urologic tissue regeneration. Many researchers have reported successfully regenerated urothelium, muscle layers, and complete vascularization in pre-clinical models while others have observed graft contracture, inflammation, and urine leakage[3,5]. These complications have been attributed to poorly matched mechanical properties; for example, poor distensibility or rapid scaffold degradation prior to urothelium regeneration[17,18]. Efforts have been made to produce dECM scaffolds for load-

bearing tissue regeneration by tuning the mechanical strength through chemical crosslinkers. However, the use of such crosslinking agents has caused increased immunogenicity and reduced scaffold elasticity, a key property required for proper bladder tissue function[19–21]. Instead, other strategies have been employed to strengthen dECMs while maintaining favourable cellular interactions. Ge et al. modified UBM scaffolds with a dopamine coating to improve scaffold strength for urological applications[22]. Improvement of strength was observed through higher break force required and reduced degradation; however, material elasticity was not tested, and scaffold strength was not contextualized in terms of the bladder. Alternatively, Roth et al. incorporated nanoparticles in SIS scaffolds to reduce their permeability and prevent urine leakage; slight improvements in smooth muscle regeneration did not serve to improve bladder capacity post-surgery[23]. In an attempt to reduce chronic inflammation and fibrosis, dECM scaffolds have been loaded with additional growth factors for slow release *in vivo*. Some inhibition of graft contracture was achieved, but no significant differences were observed in terms of tissue regeneration[24]. As such, a modified dECM scaffold that meets the aforementioned design requirements remains elusive.

Synthetic polymer hydrogels, while attractive alternatives to naturally-derived scaffolds because of their reproducibility and tunability, have been found to have limited success in the regeneration of load-bearing tissues[25]. Abdurrahmanoglu et al. demonstrated that long, hydrophobic molecules can act as transient crosslinkers that enhance energy dissipation through reversible non-covalent bonding upon addition to polymer hydrogels[26]. This phenomenon has led to the development of high strength, viscoelastic hydrogels with self-healing abilities[25,27,28]. Additionally, a study on aliphatic n-alkanols conducted by Carignan et al. concluded that the

immunomodulatory impact of these molecules is correlated with their hydrophobicity[29]. Inspired by these findings, we developed a methodology that creates elastomeric collagen gels through the integration of aliphatic chains[30]. We investigated a series of aliphatic chains of varying lengths and found a C18 hydrophobe to result in the most improvement in the compliance of naturally-derived hydrogels. We aim to test this method further using various dECMs in order to create tougher, compliant scaffolds without the use of traditional crosslinking agents. We hypothesize that the addition of aliphatic chains will improve scaffold survival *in vivo* by reducing degradation rates and promoting a pro-regenerative immune cell phenotype; in conjunction with the naturally present biological cues, these modified dECM scaffolds may be better suited to generate biomechanically functional bladder tissue. Five different dECMs were modified in this study and evaluated for further pre-clinical studies using the following design aspects: their mechanical and physical properties post-modification, their ability to support cell adhesion and proliferation, and material immunogenicity. Here, we investigate the potential for dECMs modified with C18 aliphatic chains as suitable scaffolds for bladder tissue regeneration.

2 Experimental Methods

2.1 dECM Scaffold Source

Five different dECM scaffolds from different tissue sources were chosen to be studied. None of the scaffolds chosen were crosslinked prior to purchasing. The Cook Biodesign 4-layer tissue graft was chosen to study porcine SIS and the porcine UBM scaffold studied was the ACell Matristem Bladder Matrix Sheet, both obtained from the vendor, esutures.com. The Bovine Pericardium Dural Graft was purchased from Integra LifeSciences. The Integra Surgimend 1.0 Acellular matrix and the Humend 1.0 Acellular matrix were purchased to study bovine dermis and human dermis, respectively. Both dECM materials were also procured from esutures.com.

2.2 dECM Scaffold Modification

dECM scaffolds were chemically modified using Isooctadecenylsuccinic anhydride (C18) obtained from TCI Chemicals. A C18 solution was diluted to 20 mg/mL in DMSO (Thermofisher). Prior to reaction, dECM scaffolds were soaked in PBS (pH 7.4) for 15 minutes; excess liquid was removed, and the scaffold was submerged in 20 mg/mL C18 in dimethyl sulfoxide (DMSO). Scaffold in solution was left on a rotator at room temperature for either 1 or 2 hours. After the designated reaction time, modified scaffolds were taken out of DMSO and washed 3 times in PBS for 5 minutes each wash. dECM scaffolds were also thermally denatured to further compare the mechanical properties. To do so, samples were soaked in PBS for 15 minutes at room

temperature (RT) prior to being transferred to incubated at 65^{o}C for 2 hours. Scaffolds were then left to cool at RT and dried overnight.

2.3 Mechanical Testing

Uniaxial tensile testing was performed using the MTS Criterion Model 43 and a 100N load cell with a constant strain rate of 1 mm/min. Rectangular samples of ECM (n=3 per group) and rabbit bladder tissue (n=3) were placed in a paper-based custom apparatus to provide proper grip during experiments. Sample width, length and height prior to testing were recorded and used to calculate tensile strength, material toughness and linear elastic moduli at 0-20% strain and 0-100% strain. Data was recorded and processed using Microsoft Excel, R, and Prism 8.0 software programs.

2.4 Swelling Ratio, Enzymatic Degradation and Contact Angle Measurements

Dry weights of unmodified and modified dECM scaffolds were measured for each sample (n=3 per group per material) and kept in PBS (pH 7.4) at 37^{o}C. Wet weights were measured at t=0, 1, 2, 3, 4, 6 and 24 hours. The swelling ratio of each sample was plotted over time where swelling ratio is defined as (Wet weight of sample– Dry weight of sample)/Dry weight of sample. Similarly, scaffold degradation with and without modification was analyzed in the presence of Collagenase I. Collagenase I (Worthington Biochemical Corporation) was dissolved in PBS (pH 7.4) at a concentration of 0.5 mg/mL. Dry weights were measured for each sample, left to swell in PBS for 24 hours, transferred to the enzyme solution, and kept at 37^{o}C. Wet weights of samples

were measured at t=0, 24, 48, 72, and 96 hours; data is presented as a ratio of the sample wet weight at time t to the dry weight of sample. Additionally, material wettability with and without the addition of C18 molecules was evaluated through contact angle directly measured from the drop profile. Water droplets were pipetted onto material surface and an image was taken of liquid-solid interface. The angle at this interface was measured using ImageJ angle tool. All measurements done in triplicate for each material.

2.5 Human Bladder Epithelial Cell and Fibroblast Proliferation

Human Bladder Fibroblast cells (hBFCs) were obtained from ATCC and cultured in MEM + 10% FBS + 1% P/S (Gibco). These cells were cultured until passage 4 prior to experimental use with cell culture medium exchanged every 2 days. Human Bladder Epithelial Cells (hBECs) were purchased from ATCC and cultured in Prostate Epithelial Cell Basal Medium supplemented with Corneal Epithelial Cell Growth Kit (ATCC). These cells were cultured until passage 3 on Poly (L-Lysine) (Sciencecell) coated cell culture flasks with cell culture medium exchanged every 2-3 days.

Unmodified and C18-modified dECM scaffold were cut into 7-mm diameter scaffolds using a biopsy punch and left to swell in PBS overnight. Samples were then submerged in 0.1 M $NaHCO_3$ for 24 hours. This was then followed by sterilization using a peracetic acid treatment (0.2% peracetic acid, 4% ethanol) for 4 hours followed by 3 PBS washes of 1 hour each. Once samples were placed in designated wells of 96 well plate, 200 µL of complete media was added to each well for overnight incubation prior to cell seeding.

hFBCs at passage 4 and hBECs at passage 3 were detached with trypsin (0.25%, 3 mL per T25 flask), spun down at 1000 rpm for 5 minutes, and resuspended in media to approximately 4x105 cells/mL. Approximately 2000 cells or 5 µL of the cell suspension were added to 150 µL of fresh media in each well and cultured for 1, 3, and 5 days at 37°C, 5% CO_2 to evaluate cell-material interactions through direct contact. Media was exchanged every day. Cell number was evaluated at each time point using the CellTiter-Glo 3D Cell Viability assay (Promega) according to manufacturer's instructions.

2.6 Immunomodulation *in vitro*

2.6.1 Monocyte to macrophage differentiation

Monocyte culture, differentiation and macrophage polarization were performed in accordance to an earlier published protocol by Zarif et al[31]. Human THP-1 monocytes (ATCC) were cultured in RPMI-1640 medium + 10% FBS + 1% P/S. Monocytes were counted every 3 days to ensure the cell density remained between 0.2-1.0 x 10^6 cells/mL. Monocytes were cultured until passage 12-14 prior to experimental use. dECM samples (control and modified) were prepared in a similar manner to fibroblast adhesion and proliferation studies. After sterilization and subsequent washing, samples were placed in designated wells of a non-tissue culture treated 24-well plate with 500 µL of RPMI-1640 + 10% HI-FBS + 1% P/S and incubated overnight prior to cell seeding.

Monocytes were collected and spun down at 1000 rpm for 5 minutes then resuspended in RPMI-1640 + 10% HI-FBS + 1% P/S + 100 nM phorbol 12-myristate 13-acetate (PMA,

Peprotech). Approximately $0.2x10^6$ monocytes from the cell suspension were added to each well with or without dECM samples and incubated for 24 hours to promote macrophage differentiation. Subsequently, media containing PMA was removed, replaced with media without PMA and cultured for an additional 48 hours prior to harvesting for further analysis. Macrophages cultured on tissue culture plate were used as reference for gene expression analysis.

2.6.2 Macrophage Polarization

Control 2D cultures were also seeded in wells not containing dECM samples. Additional 2D cultures were biochemically stimulated into an "M1" or "M2" phenotype using the following treatment. In addition to PMA, 20 ng/mL of GM-CSF (M1) or M-CSF (M2) was added to the culture medium. After 24 hours, media was exchanged for RPMI-1640 + 10% HI-FBS + 1% P/S + 20 ng/mL GM-CSF or M-CSF and incubated for another 24 hours. Media was once again removed from macrophages and replaced with RPMI-1640 + 10% HI-FBS + 1% P/S + M1 or M2 polarizing cytokines obtained from Peprotech: specifically, 20 ng/mL LPS (Sigma), IFN-γ, GM-CSF and IL-6 for M1 polarization and 20 ng/mL of IL-4, Il-13, M-CSF and IL-6 for M2 polarization. Macrophages were left to incubate in cytokine-enriched media for 72 hours prior to harvesting for further analysis.

2.6.3 Gene Expression by RT-qPCR

Relative gene expression levels were assessed for harvested samples 48 hours after PMA removal. 500 µL of TRIzol (Invitrogen) added to each well, triturated and incubated for 5 minutes.

TRIzol solution and ECM scaffold sample were transferred to centrifuge tube and kept at -80^{o}C for at least 24 hours. Samples were later thawed to RT and chloroform extraction performed for total RNA isolation. In brief, 100 µL of chloroform (Sigma) was added to each tube and the solution was shaken vigorously for 15 sec followed by a 3-minute incubation and centrifugation at 12000g for 15 min at 4^{o}C. The upper phase was collected and 250 µL isopropanol (Sigma) to precipitate RNA, incubated for 10 min and centrifuged at 12000g for 10 min at 4^{o}C. The supernatant was removed, followed by two pellet washes using 75% EtOH (Sigma). RNA Pellets were air-dried and resuspended in nuclease-free water. Total RNA content measured using the Nanodrop One spectrophotometer (Thermofisher). RNA was subjected to RT-qPCR using primers specified for gene of interest and AgPath-ID One step RT PCR Universal Mix (Thermofisher) in a total volume of 12 µL per reaction. Samples were run in triplicate in a 384-well plate along with the housekeeping gene as controls. RT-PCR was performed using comparative C_T Applied Biosystems at the following cycle conditions: Hold at 45°C for 10 min and at 95°C for 10 min followed by 40 cycles of denaturing at 97°C for 2 seconds and annealing at 60°C for 30 seconds each cycle. A delta delta C_T method was used to analyze the data points. The following genes were assessed using TaqMan's RT-qPCR primers/probe set: Transforming growth factor β1 (TGFβ1), tumor necrosis factor α (TNFα), CD86, CD163, CD68, and ubiquitin C (UBC) as the housekeeping gene.

2.7 Biocompatibility *in vivo*

2.7.1 Subcutaneous implantation

Animal studies were performed in accordance to protocols approved by the Johns Hopkins University Hospital Animal Care and Use Committee. Sprague Dawley white rats (2 male, 2 female – 8 to 12 weeks) were anaesthetized using isofluorane and 4 samples (5mm x 5mm size) of control dECM and modified dECM samples were grafted in the anterior ventral side of the rats. Incisions were cut on the dorsal section through the skin and scaffolds were implanted over the muscle under the skin. The incisions were sutured using Surgipro II monofilament polypropylene 6-0 (Covidien). The rats were then split into two groups by time point, 7 days and 21 days respectively. At each time point, the rats were sacrificed, and the grafts harvested for histological analysis.

2.7.2 Histological and Immunostaining

Haematoxylin and eosin (H+E) staining was used to evaluate cell infiltration and Masson's trichrome staining was performed to observe collagen content over time. All staining procedures were performed on formalin fixed, paraffin embedded tissues. Tissues were sectioned at 6 μm thickness and placed on glass microslides. H+E and Masson's trichrome staining was performed by a research specialist at the Department of Pathology, Johns Hopkins University. Images taken at 20x magnification were processed using ImageJ to determine number of cells/mm^2 in the

center of the scaffold at each time point and thickness of collagen deposition at the biomaterial-muscle interface at Day 21.

2.8 Statistical analysis

Unpaired t-test with Welch's correction was performed to determine and statistical significance in mean values unless stated otherwise (n=3). Statistically significant values ($p<0.05$ or $p<0.01$) were marked as * or **, respectively.

3 Results

3.1 Mechanical Testing

The mechanical properties of all unmodified dECM scaffolds, samples modified with C18 aliphatic chains for 1 h and 2 h, as well as thermally denatured samples were evaluated through uniaxial tensile testing; rabbit bladder tissue was also tested for comparison. From tensile curves (Figure 1 depicts representative sample curves), peak values, elastic moduli and toughness were calculated and are summarized in Table 1. Rabbit bladder tissue exhibited a peak stress of 0.48 $\pm$ 0.2 MPa and achieved 122 $\pm$ 38% elongation at this point; thus, a reference point of 100% elongation at 0.4 MPa was used to compare modified dECM samples to native bladder tissue in order to evaluate any changes in material elasticity.

In general, the characteristic *J*-curve of viscoelastic materials was maintained for both modified and denatured materials (Figure 1). Modified porcine SIS showed considerable improvement in compliance at low stress values. The material elongation achieved at 0.4 MPa increased from 15% for unmodified SIS to approximately 45% for both C18-modified scaffolds tested (Figure 1B). All modified SIS scaffolds showed reduced elastic moduli from 0-20% and 0-100%, indicating higher compliance. Longer reaction time increased material toughness and reduced compliance. A higher variability in peak stress was observed with minimal change in material toughness relative to the control: 846 $\pm$ 158 J/m^3 for unmodified, 761 $\pm$ 67 J/m^3 for 1 h reaction and 832 $\pm$ 333 J/m^3 for 2 h reaction. In contrast, thermally denatured samples had a toughness of 647 $\pm$ 684 J/m^3 .

Modified porcine UBM displayed elongated *J*-curves (Figure 1C), further characterized in Table 1. The 1 h modified UBM had a lower elastic modulus at both 20% and 100% strain, 1.35 ± 0.47 MPa and 1.87 ± 0.43 MPa respectively, compared to unmodified UBM with 2.03 ± 1.04 MPa and 3.11 ± 0.43 MPa. The largest peak strain was achieved by the 2 h C18 modified UBM; however, only the 0-100% elastic modulus was reduced at 1.64 ± 0.21 MPa. Thermal denaturation severely compromised material integrity as seen in the 6-fold reduction in toughness (51 ± 14 J/m^3). C18 modification of UBM resulted in moderate, but insignificant, increase in material toughness.

Bovine pericardium benefited the most from the incorporation of hydrophobes with an overall reduced peak stress (2.86 ± 1.0 MPa for unmodified, 1.62 ± 0.4 MPa for 1 h reaction time and 1.23 ± 0.4 MPa for 2 h reaction time) and at least a 1.5-fold increase in strain achieved at peak stress (197 ± 33% for unmodified, 333 ± 55% for 1 h reaction time and 409 ± 89 % for 2 h reaction time). At 0.4 MPa, unmodified bovine pericardium reached a 40% strain while samples modified with C18 for 2 hours reached 125% strain, a value very similar to rabbit bladder tissue (Figure 1D). The thermally denatured material exhibited improved distensibility that was on par with modification; a drastic decrease in overall toughness from 290 ± 257 J/m^3 to 84 ± 33 J/m^3 called material stability into question. Aliphatic chain modification also reduced the variability reported in control pericardium toughness: 355 ± 178 J/m^3 for a 1 h reaction and 310 ± 159 J/m^3 for a 2 h reaction.

Bovine dermis also responded well to aliphatic chain modification. A modest increase in strain at 0.4 MPa (80% for unmodified, 110% for 1 h C18-modified, 140% for 2 h C18-modified) resulted in values more similar to bladder tissue (Figure 1E). Higher overall toughness values of

395 ± 138 J/m^3 for unmodified, 1071 ± 844 J/m^3 for 1 h reaction time and 636 ± 139 J/m^3 for 2 h reaction time indicated a vast increase in material strength. Interestingly, the properties of bovine dermis were heavily affected by thermal denaturation, displaying very mechanically weak, gelatin-like behavior with peak stress values of 0.09 ± 0.1 MPa and toughness of 3 ± 2 J/m^3.

Unmodified human dermis displayed a more viscoelastic curve than other dECM scaffolds tested (Figure 1F). The largest final elongation of all materials was achieved with the 2 h modified human dermis at 673 ± 198% while unmodified human dermis had a final strain of 417 ± 106% and a moderate increase was observed with human dermis modified with C18 for 1 hour (580 ± 78%). Interestingly, the final elongation of thermally denatured human dermis was on par with the 2 h modified samples at 648 ± 150%. C18 modification improved the elongation as well as resulted in a higher peak stress. Reaction time did not have a significant effect on human dermis mechanical properties. The elastic moduli of modified material were found to be similar to those of bladder tissue. Thermally denatured human dermis appeared to be more intact compared to other dECMs after the same modification as demonstrated by its capacity to elongate 528 ± 139% at peak stress of 4.06 ± 0.8 MPa. Overall, C18 modified human dermis improved material toughness and stiffness to more closely match bladder values.

In general, C18 modification was found to not only improve scaffold elasticity for all dECMs included in this study, but also improve material strength overall. These improvements to the mechanical properties of naturally derived scaffolds address a primary concern for bladder tissue regeneration that has been previously overlooked, specifically the poor distensibility found to be common in dECMs.

Table 1. Summary Values from uniaxial tensile testing: Uniaxial tensile testing was performed at constant strain rate of 1.0 mm/min. Peak stress and strain, final elongation achieved, elastic modulus calculated from 0 to 20% and from 0 to 100% strain shown. The area under the stress-strain curves was used to quantify material toughness. TD = Thermally Denatured at 65°C.

dECM	Modification	Peak Strain		Peak Stress		Final Strain		0-20 % E		0-100% E		Toughness	
		%		MPa		%		MPa		MPa		J/m^3	
		Mean	SD	Mean	SD	Mean	SD	Mean	SD	Mean	SD	Mean	SD
Rabbit Bladder		122	38	0.48	0.2	224	145	0.53	0.35	0.34	0.10	67	61
	Unmodified	194	49	5.18	0.7	315	49	1.82	1.20	3.13	1.04	846	158
Porcine	C18 1 h rxn	317	73	3.98	0.4	370	57	0.96	0.82	1.09	0.49	761	67
SIS	C18 2 h rxn	311	24	4.92	2.4	343	37	1.34	0.82	1.26	0.69	832	333
	TD	165	70	5.09	2.9	222	85	0.79	0.48	2.90	0.73	647	684
	Unmodified	101	23	3.75	0.8	145	18	2.03	1.04	3.11	0.43	261	70
Porcine	C18 1 h rxn	170	24	3.23	0.1	206	61	1.35	0.47	1.87	0.43	321	87
UBM	C18 2 h rxn	191	29	2.97	0.4	209	27	2.20	0.74	1.64	0.21	329	79
	TD	136	11	0.69	0.1	177	38	0.25	0.12	0.48	0.14	51	14
	Unmodified	197	83	2.86	1.0	280	113	0.39	0.37	0.74	0.11	290	257
Bovine	C18 1 h rxn	333	55	1.62	0.4	426	101	0.49	0.21	0.46	0.15	355	178
Pericardium	C18 2 h rxn	409	98	1.23	0.4	461	110	0.42	0.27	0.35	0.07	310	159
	TD	323	115	0.47	0.1	441	160	0.12	0.02	0.13	0.09	84	33

	Unmodified	411	96	1.65	0.3	499	74	0.17	0.05	0.31	0.13	395	138
Bovine	C18 1 h rxn	519	255	2.95	1.5	567	271	0.54	0.53	0.63	0.33	1071	844
Dermis	C18 2 h rxn	496	78	2.19	0.4	558	101	0.48	0.58	0.53	0.43	636	139
	TD	35	14	0.09	0.1	91	23	0.17	0.05	0.01	0.00	3	2
	Unmodified	289	81	2.16	1.0	417	106	0.05	0.03	0.24	0.16	339	143
Human	C18 1 h rxn	447	36	3.62	0.4	580	78	0.44	0.36	0.45	0.28	996	260
Dermis	C18 2 h rxn	523	47	3.33	0.5	673	198	0.34	0.07	0.39	0.12	1208	742
	TD	528	133	4.06	0.8	648	150	0.02	0.01	0.04	0.02	1100	232

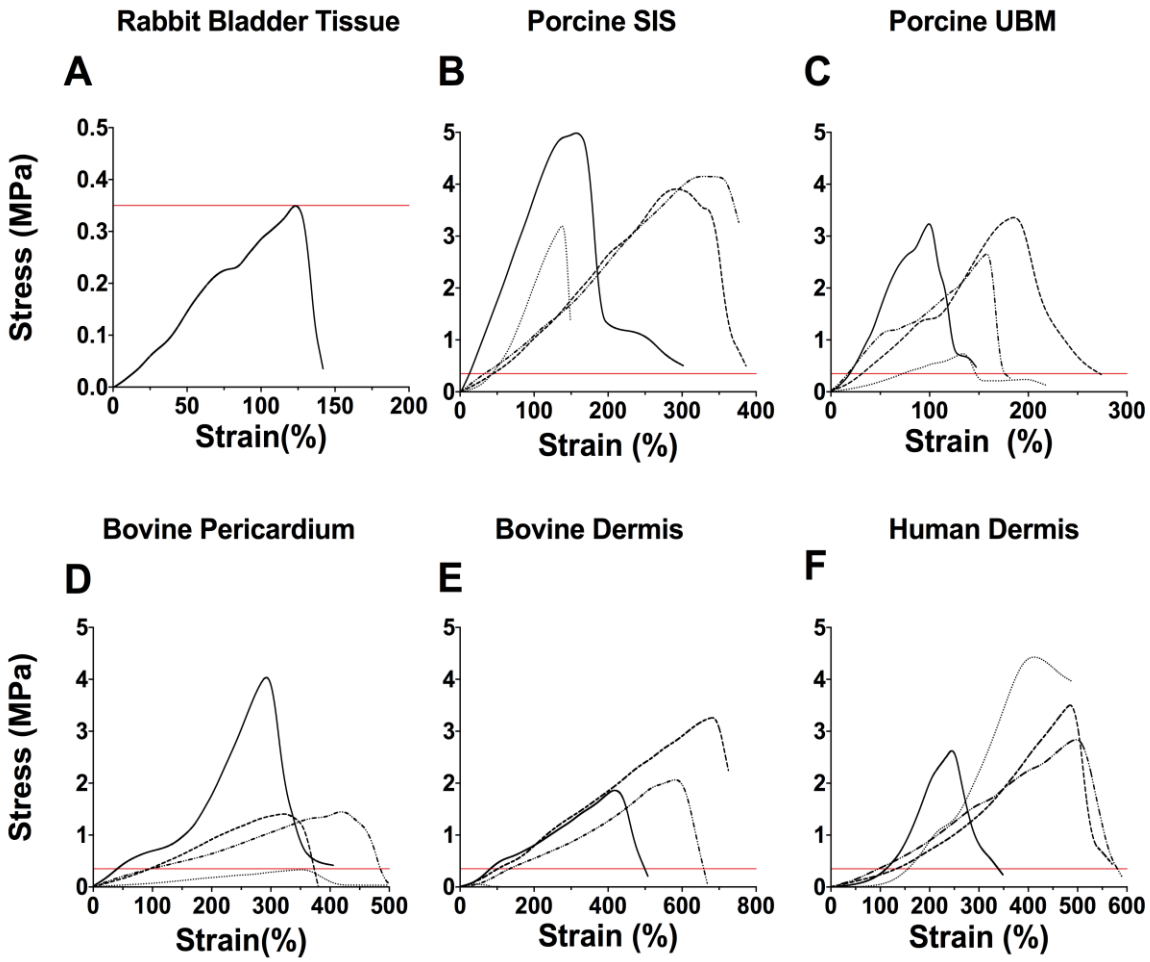

Figure 1. Uniaxial tensile strength of control and modified dECM: Tensile tests were evaluated at room temperature with constant strain rate of 1.0 mm/min. Rabbit tissue bladder (**A**) was tested for comparison. Representative tensile stress vs. strain of porcine SIS (**B**), porcine UBM (**C**), bovine pericardium (**D**), bovine dermis (**E**),and human dermis (**F**) are shown as follows: dECM scaffolds(unmodified ——), dECM modified with C18 molecules for 1 hour (C18 1h rxn – –), dECM modified with C18 molecules for 2 hours (C18 2h rxn —••) and thermally denatured dECM (65^{o}C 2 h •••).

3.2 Swelling and Enzymatic Stability

The effect of aliphatic chain modification and thermal denaturation of dECM scaffolds on their swelling was investigated at 37°C (Figure 2A-E), as well as on their degradation profiles in the presence of 0.5 mg/mL Collagenase I (Figure 2F-J). In general, the addition of C18 molecules had no significant effect on the swelling profile at t=0, 1, 2, 3, 4, 6 h for all materials tested. Scaffold modification had no significant effect on the swelling ratio over time for porcine SIS. Differences in the swelling ratio were observed at t=24 h in porcine UBM, bovine pericardium, and human dermis. Thermal denaturation resulted in an increased swelling ratio for porcine UBM while C18 modification resulted in similar profiles for both reaction times tested; at t=24 h, a lower swelling ratio of 91 ± 16% was observed for 1 h reaction time while samples modified for 2 h had a swelling ratio of 160 ± 59% (Figure 2B). Bovine pericardium and bovine dermis scaffold behavior changed significantly upon thermal denaturation with much higher swelling ratios compared to other samples at all time points. Thermally denatured bovine pericardium achieved a final swelling ratio of 617 ± 38% at t= 24 hours compared to 276 ± 16% for the unmodified scaffold (Figure 2C). Material degradation was observed for thermally denatured bovine dermis (Figure 2D), as shown in the swelling ratio decline between 6 h (430 ± 51%) and 24 hours (160 ± 110%). In contrast, thermal denaturation did not affect swelling over time for human dermis; C18-modified scaffolds showed slight reduction of water intake relative to unmodified human dermis. Thus, the addition of C18 aliphatic chains did not significantly affect material swelling over time and modified scaffolds were able to maintain structure at a physiologically relevant

temperature. Heat exposure resulting in protein denaturation was found to negatively affect dECM thermal stability.

Across all dECM scaffolds tested, with the exception of human dermis, both unmodified and thermally denatured samples exhibited complete degradation within 24 hours. C18-modified SIS samples were able to withstand exposure to Collagenase I for over 96 h with little change in weight. Porcine UBM modified with C18 molecules for 2 h was the only sample of UBM to demonstrate delayed digestion. Relative to other tissue sources, bovine pericardium exhibited the highest degradation across modified and unmodified. However, while unmodified and thermally denatured had been completely digested within 24 h, some material was salvageable for wet weight measurements for C18-modified scaffolds. Longer reaction time improved material stability, most noticeably for porcine UBM with wet weight to dry weight ratio of 2.1 ± 0.43 after 24 h and bovine pericardium at a ratio of 1.5 ± 1.0 after 24 h of enzymatic digestion. Bovine dermis exhibited similar behavior as porcine SIS, with a 25% reduction in wet weight loss by t=96 h. Human dermis samples exhibited the highest resistance to collagenase I with the addition of C18 chains further improving collagenase resistance; heat denaturation resulted in steady degradation of the dECM over time.

Overall, the addition of aliphatic chains improved resistance to protease degradation while maintaining a similar swelling profile for all tissue types included in this study. The findings of this experiment indicate that C18 modification may serve to delay material degradation *in vivo* and support the slow process of urothelium regeneration for a longer period of time. Based on this information, *in vitro* and *in vivo* studies were conducted on best performing modified material and unmodified dECM. A one-hour reaction time was chosen for porcine SIS and human dermis,

while a two-hour reaction time was selected for porcine UBM, bovine pericardium and bovine dermis.

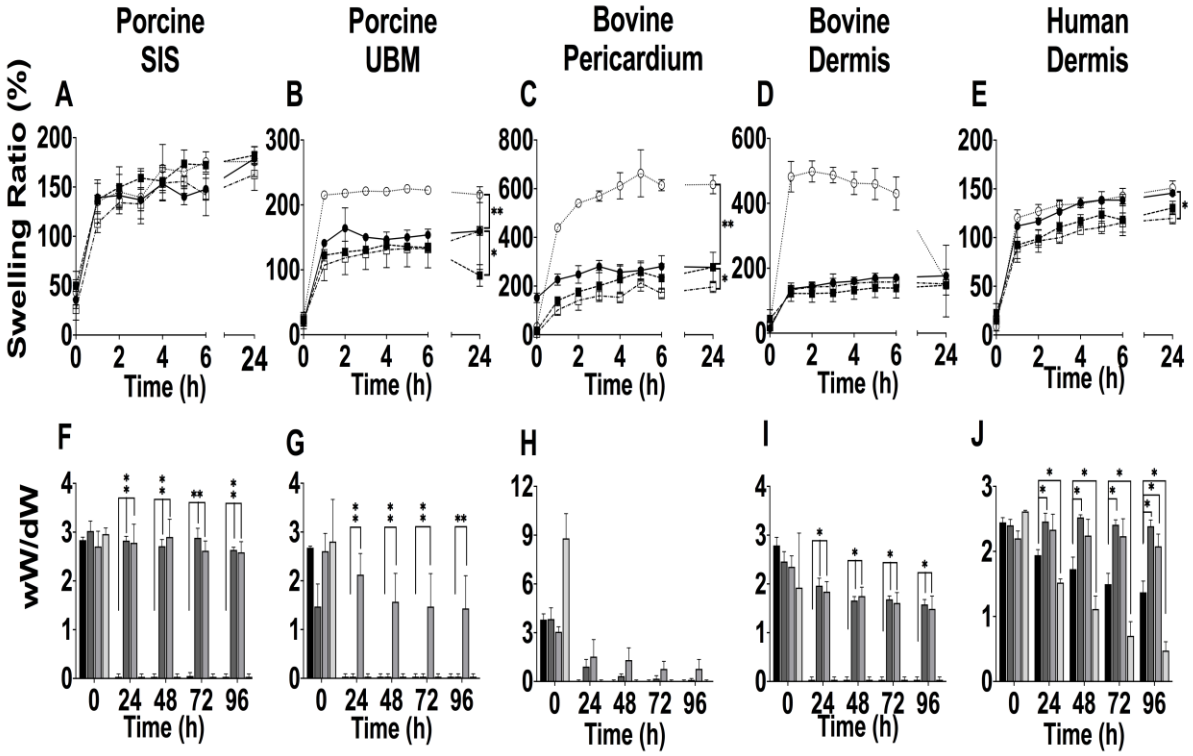

Figure 2. Evaluation of swelling behavior and resistance to enzymatic degradation with and without aliphatic chain modification: Swelling Ratio of unmodified and modified dECM scaffolds at 37^{o}C, pH 7.4 (**A-E**) Groups shown for each dECM are as follows: dECM scaffolds (unmodified ●), dECM modified with C18 molecules for 1 h (C18 1h rxn ■), dECM modified with C18 molecules for 2 hours (C18 2h rxn □) and thermally denatured dECM (65^{o}C 2 h ○). Weight of unmodified and modified dECM scaffolds remaining in 0.5 mg/mL collagenase I was also measured over time (**F-J**). Groups shown for each dECM are as follows: dECM scaffolds (unmodified ▬), dECM modified with C18 for 1 h (C18 1h rxn ▭), dECM modified with C18 for 2 h (C18 2h rxn ▭) and thermally denatured dECM (65^{o}C 2 h ▭).

3.3 Surface Hydrophobicity and Direct Cell Adhesion

Surface hydrophobicity was evaluated before and after modification using contact angle measurements (Figure 3A). All dECM scaffolds tested showed an increase in surface hydrophobicity after the addition of aliphatic chains, as expected. Unmodified porcine SIS was the only dECM studied to display hydrophilicity (Contact angle < 40^o); after 1 h modification, SIS shifted toward moderate hydrophobicity (48^o < Contact angle < 62^o)[32].

Interestingly, human bladder fibroblast growth was highest in direct contact with control porcine SIS scaffolds contact at 4.3 $\pm$ 1.8 fold increase in cell number by Day 5 (Figure 3B). Modified porcine SIS showed initial cell adhesion support, but no significant change in cell number was observed over time. Cell growth was also evaluated for human bladder epithelial cells and THP-1 activated macrophages on porcine SIS scaffolds to observe the effect of increased hydrophobicity on different cell types (Figure 3C). Macrophage adhesion did not differ significantly between control and modified SIS materials. In contrast, epithelial cells attached preferably to the modified porcine SIS scaffold. Epithelial cell behavior was also observed over time for all scaffolds (Figure 3D). Porcine SIS control samples initially allowed for epithelial cell adhesion at t=24 h; growth was not supported as shown with stagnant or lower cell numbers at t=72 h and 120 h.

Unmodified materials that display moderate wettability (namely porcine UBM, bovine pericardium and human dermis) were classified as extremely hydrophobic after the addition of aliphatic chains. Unmodified UBM and pericardium also had some ability to support fibroblast adhesion over time. The number of cells did not change over time for UBM considerably over time; a 3.3 $\pm$ 0.8 -fold increase in cells from initial seeding (N/N_0) for bovine pericardium indicated

that the material is better able to sustain fibroblast growth. Increased hydrophobicity reduced cell adhesion capacity for both scaffolds; this is more noticeable at 72 h and 120 h where few, if any, cells are detected. This behavior was not consistent with epithelial cells. Initially, few cells are found on unmodified Porcine UBM ($N/N_0 = 0.06 \pm 0.05$); cell growth is delayed with N/N_0 marginally increasing to 1.3 ± 0.9. Initial cell values were comparable for modified UBM scaffolds, with substantially less recovery in cell number observed by 120 h at $N/N_0 = 0.20 \pm 0.08$. Epithelial cells adhered well to bovine pericardium control samples ($N/N_0 = 1.2 \pm 0.2$ at t = 24 h); however, a gradual decrease was observed over time. The number of cells did not change over time for C18-modified bovine pericardium samples.

Although human dermis scaffolds were found to have comparable wettability to porcine UBM and bovine pericardium, neither control nor modified samples supported fibroblast growth. Epithelial cell adhesion was moderately improved relative to fibroblasts with $N/N_0 = 0.10 \pm 0.01$ and $N/N_0 = 0.12 \pm 0.04$ for control and C18-modified samples, respectively. Bovine dermis was found to be the most hydrophobic material, with the highest contact angle of all ECM scaffolds tested, both before (77 ± 8^o) and after C18 modification (102 ± 5^o). Regardless, fibroblast adhesion is detected on day 1 and a 2.5 ± 0.9-fold increase in cell number is observed in bovine dermis control samples. Cell growth is considerably delayed on modified bovine dermis. Similarly, epithelial cell adhesion was maintained at t=24 h and t=72 h on control bovine dermis samples while few cells adhered to modified bovine dermis at all time points.

While the ability to support cell growth varied by dECM source, the increased hydrophobicity of C18-modified materials caused reduced bladder fibroblast proliferation over

time. Moderately hydrophobic materials supported bladder epithelial cells; few epithelial cells were detected on extremely hydrophilic or hydrophobic dECM scaffolds.

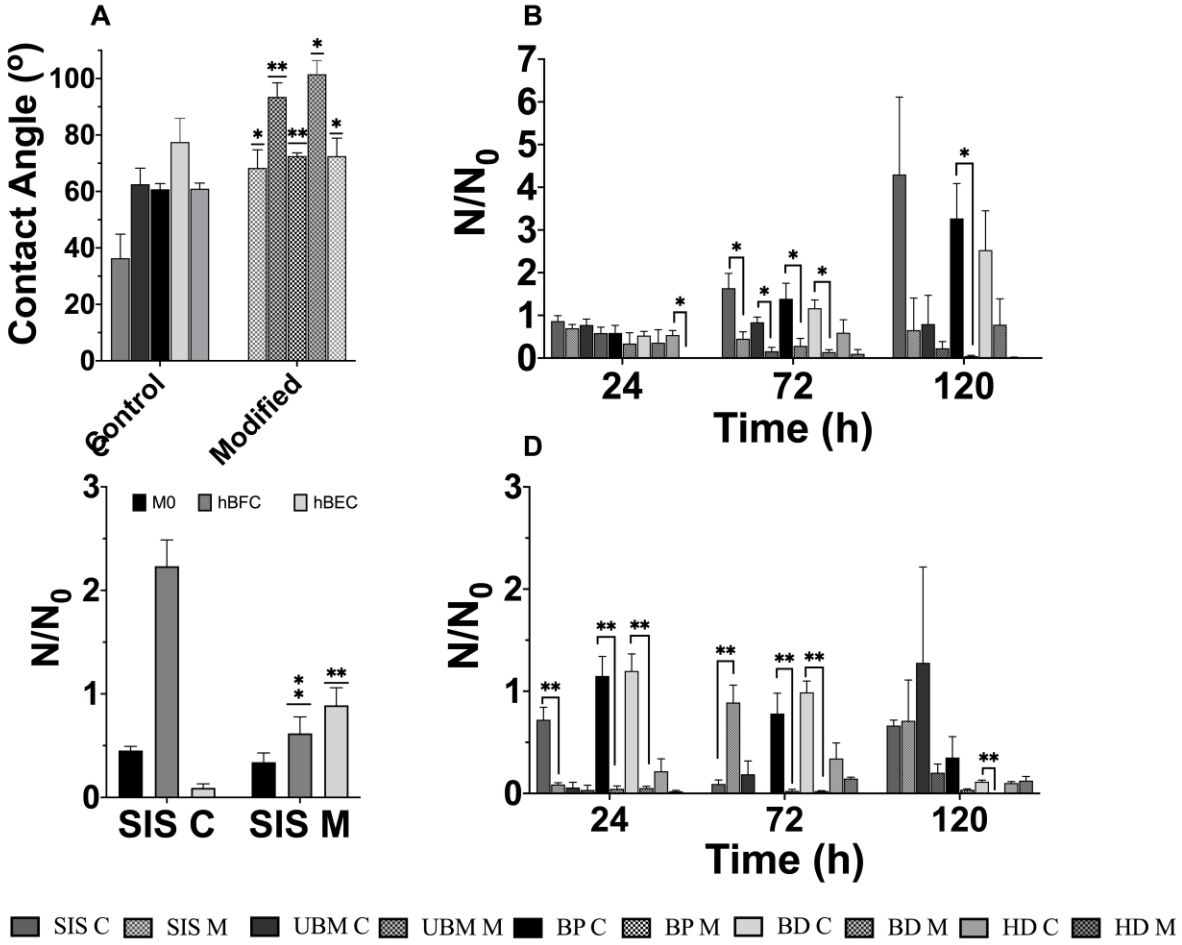

Figure 3. Hydrophobicity and cytotoxicity *in vitro*: A) Surface hydrophobicity assessed through direct measurement of water-material contact angle. C18 modified samples exhibit higher contact angle, signifying increased hydrophobicity. **B)** human bladder fibroblast growth determined through luciferase assay at t= 24, 72, 120 h for control dECM and modified dECM as chosen based on mechanical and physical properties. **C)** The effect of C18 modification on cell adhesion was compared between SIS control and modified for activated macrophages (M0), human bladder fibroblasts (hBFCs) and human bladder epithelial cells (hBECs) at t=72 h. **D)** human bladder epithelial cell growth was also determined through luciferase assay at t= 24, 72, 120 h for control and modified dECM. All cell numbers were normalized to initial cell seeding density (2000 cells/well).

3.4 Immunomodulation *in vitro*

The short-term immune response was investigated *in vitro* by differentiating THP-1 monocytes to macrophages in the presence of control or modified dECM scaffolds, followed by RNA isolation and gene expression analysis for *CD68* (M0 surface marker), *CD86* ("M1" surface marker), *CD163* ("M2" surface marker), *TNF-*α (pro-inflammatory cytokine), and *TGF-*β (anti-inflammatory cytokine).

Biochemically stimulated macrophages were also evaluated for expression of the above genes. Interestingly, differences in surface marker expression were noticeably observed between polarized macrophages and unpolarized macrophages (Figure 4). M-CSF + LPS + IL-6 + IFN-γ stimulation to generate M1 polarized macrophages caused a significant increase in CD68 and CD86 expression with no change in CD163 or TNF-α. A decrease in TGF-β was observed. GM-CSF + IL-4 + IL-13 + IL-6 stimulation for the M2 polarized macrophages showed no change in CD68 expression, reduced CD86, TNF-α and TGF-β as well as very high expression of CD163. In contrast, significant changes between different tissue sources as well as between control and C18-modified scaffolds were observed in cytokine expression with a reduced or minimal effect on surface marker expression (Figure 5).

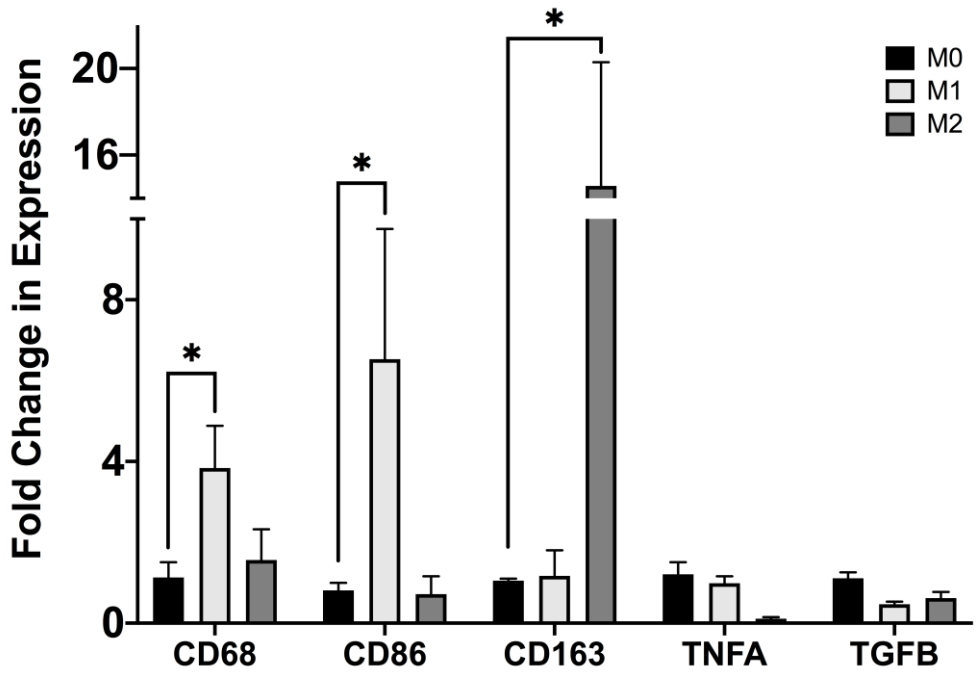

Figure 4. Surface Marker expression of biochemically polarized macrophages: Gene expression analysis using RT-qPCR of macrophages exposed to pro-inflammatory (M1) or anti-inflammatory (M2) cytokines. Biochemically stimulated macrophages showed upregulation in corresponding surface marker (M1-CD86 and M2-CD163) compared to control (M0) but no significant differences observed in cytokine expression.

The normalized fold change of expression for each gene of interest and dECM experimental group relative to 2D M0 expression is shown in Figure 5. Macrophages cultured with unmodified porcine SIS maintained expression levels of CD163 and TNF-α and downregulated expression of CD68, CD86 and TGF-β relative to 2D controls, suggesting a "mixed" macrophage phenotype. CD68 expression levels comparable to 2D controls was found in modified SIS samples with no change in CD86 and slight increase in CD163 compared to control SIS samples. TNF-α expression was reduced in C18-modified SIS while TGF-β expression levels

increased compared to control SIS (Figure 5), indicating a shift towards an M2-like phenotype. Porcine UBM displayed similar behavior to SIS in that a downregulation of markers indicative of pro-inflammatory phenotype was observed in modified samples compared to control. CD68 levels were maintained across control UBM, modified UBM and 2D controls. Macrophages incubated with control UBM showed a high increase in CD86 and a slight increase in CD163 compared to 2D controls; CD86 levels were reduced in C18-modified porcine UBM while CD163 levels were comparable to that of unmodified UBM. Macrophage exposure to scaffolds *in vitro* resulted in an increase in cytokine expression levels. TNF-α expression was reduced upon aliphatic chain modification while TGF-β was somewhat upregulated.

Modulation of the THP-1 macrophage phenotype was seen most noticeably with bovine pericardium. CD68 expression was moderately upregulated in both control and modified scaffolds; higher expression was found for macrophages cultured with modified bovine pericardium. CD86 expression was unchanged in both samples; CD163 levels were higher than control 2D macrophages and macrophages exposed to other dECMs. TNF-α expression was maintained and higher TGF-β was observed in control bovine pericardium; in contrast, expression of TNF-α in C18-modified samples was significantly downregulated relative to both control bovine pericardium and 2D controls. TGF-β expression was also upregulated to a higher degree in modified bovine pericardium compared to its unmodified counterpart.

Macrophage differentiation was not well supported on dermis samples. Bovine dermis samples showed downregulation of all surface marker expression but very high TNF-α expression and some expression of TGF-β. Unmodified bovine dermis elicited very high response in TNF-α production, although minimal CD86 marker expression was detected. TNF-α expression was

reduced, and TGF-β levels were maintained with the incorporation of hydrophobes. A similar response was observed for human dermis dECM in terms of surface marker expression levels. However, minimal expression was detected for TNF-α in both control and modified human dermis samples. TGF-β expression was upregulated in control human dermis compared to 2D M0 controls but, unlike all other dECMs, a downregulation in TGF-β levels was seen in modified human dermis.

In general, gene expression of key macrophage phenotype markers varied across its spectrum by tissue source. However, C18 modification was shown to modulate macrophage response to the biomaterial by minimizing a severe inflammatory response and causing a shift towards a pro-regenerative (M2) phenotype. This change was observed primarily in changes in cytokine production levels rather than surface marker expression.

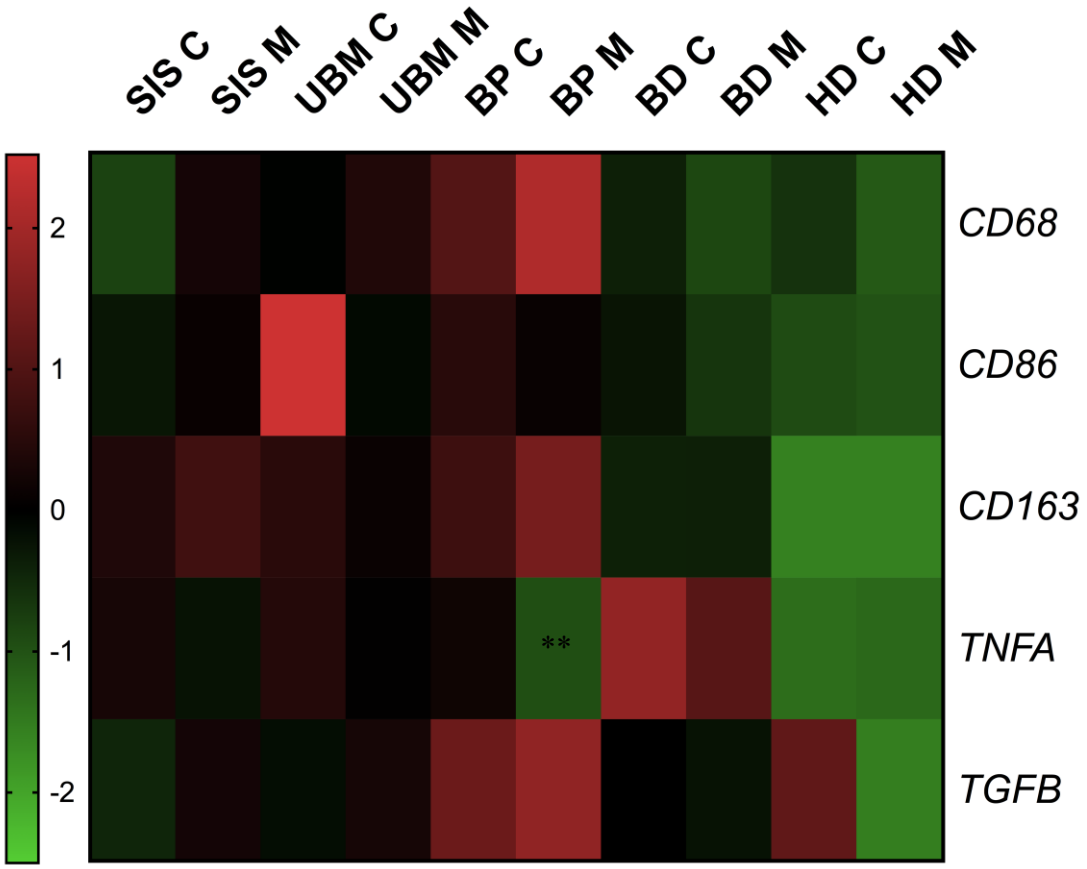

Figure 5. Macrophage polarization *in vitro*: Gene expression analysis using RT-qPCR of THP-1 macrophages exposed to unmodified and modified dECMs for 72 hours. Modified dECM showed decreased expression of pro-inflammatory genes (CD86, TNFA) while maintaining or upregulating expression of pro-regenerative markers (CD163, TGFB). CD68 was included as indicator for the presence of macrophages. All material results relative to macrophages cultured on tissue culture plastic.

3.5 Biocompatibility *in vivo*

Unmodified and C18 modified dECM scaffolds were subsequently grafted in male and female rats subcutaneously to further investigate the effect of aliphatic chain incorporation on cell-material interactions and material degradation *in vivo*. Scaffolds were harvested at Day 7 and Day 21 to observe any changes in host reaction over time. Cell infiltration was evaluated through H&E staining (Figure 6) qualitatively and quantitatively at both timepoints. Masson's Trichrome

staining was done to observe collagen content (Figure 7). Material degradation was assessed qualitatively at both time points and collagen deposition by surrounding fibroblasts at the biomaterial-muscle interface was evaluated quantitatively for Day 21 samples. Of note, differences in staining were observed in modified materials compared to control samples where C18 modification was easily observed as bright red tissues in samples stained with Masson's Trichrome. During this process, tissues are stained first with acid dye that binds to acidophilic tissue components, such as the C18 molecules, followed by an additional acid wash where the "red" color is maintained for less permeable tissues[33].

Cell infiltration throughout the unmodified porcine SIS samples as well as blood vessel formation was seen by day 7 (Figure 6A). Continued cellular presence was observed in Day 21 samples. This was confirmed in quantification of cells in the center of the material (3031 ± 1227 cells/mm^2 for Day 7 and 3099 ± 1819 cells/mm^2 for Day 21). Female rats exhibited higher cell counts relative to male counterparts at both time points. Porcine SIS also exhibited fast degradation *in vivo* (Figure 7A). Some newly deposited collagen was found in grafts harvested on Day 21; thickness of deposited layer measured to be 64 ± 33 μm with male grafts exhibiting higher collagen amounts at the interface. C18 modification noticeably affected cell infiltration for porcine SIS. High cell accumulation was observed at the edges and in between layers of the biomaterial by Day 7 (4308 ± 1316 cells/mm^2) relative to the control, although insignificant. Interestingly, samples grafted in male rats showed higher cell counts than female samples (Figure 6B). By Day 21, nuclei were observed throughout the biomaterial and accumulation at the edges was no longer found. This is evident in reduced cell counts for modified SIS at this time (2522 ± 557 cells/mm^2). Cell infiltration was, therefore, not significantly changed by the addition of

hydrophobes in porcine SIS. Material degradation rate was affected by hydrophobe modification, as seen in modified SIS samples shown in Figure 7A. The dECM was significantly more intact at Day 7 than control samples, with the bright red staining suggesting the presence of C18 hydrophobes in the scaffold. The surface modification was not observed in Day 21 modified SIS samples; although, a dense blue layer of collagen was seen. Thickness of this layer was found to be 67 ± 41 μm, comparable to control samples at this time point (Figure 7B).

Porcine UBM also experienced cell infiltration throughout the material at 3894 ± 1155 cells/mm^2, which was relatively intact at Day 7; cell presence was still found at the Day 21 time point, along with blood vessel formation in Figure 6A. Similar to porcine SIS, a slight decrease in cell counts was observed at Day 21 (2872 ± 1128 cells/mm^2). Male and female rats showed similar response in terms of cell infiltration in the biomaterial. A thick, lightly packed layer of collagen is easily seen in Trichrome stains of unmodified UBM in Figure 7A. A divergence in the amount of collagen deposited at the interface between males and females was observed by Day 21 where the thickness of the collagen layer was 2.5-fold lower in females than males (Figure 7B). The average thickness was determined to be 83 ± 47 μm, much higher than all other dECM samples. A high accumulation of cells is once again observed at the periphery of the C18 modified porcine UBM at Day 7 in Figure 6A; however, few cells are found beyond the interface into the center of the biomaterial at 290 ± 282 cells/mm^2. This is in stark contrast to the behavior observed in control samples. This delayed material breakdown and cell infiltration is confirmed by the increased cell presence in Day 21 modified samples (5217 ± 2618 cells/mm^2), a significant increase compared to control samples. Surface modification is very clearly bright red in modified Porcine UBM samples in Figure 7A. Laminated layers of porcine UBM were also more clearly

observed here. The bright red of C18-modified surface was no longer evident by Day 21. Newly deposited collagen was found (thickness of 67 ± 41 μm); this was lower than the control counterpart, but the difference was not statistically significant. Once again, grafts implanted in females were found to have less collagen deposited at the interface, 3-fold lower than male grafts (Figure 7B).

Cell infiltration was seen throughout the dECM scaffold with high vessel formation seen at Day 7 (Figure 6A). Number of cells per mm^2 of biomaterial was comparable to other dECMs at 2696 ± 1800 cells/mm^2. High variability was observed between male and female samples with 3.5-fold decrease in cell counts for female samples relative to male samples, as shown in Figure 6B. Cell infiltration at day 21 is comparable to Day 7 at 2534 ± 1315 cells/mm^2. Bovine pericardium rapidly degraded *in vivo*; This is observed observed in grafts harvested on Day 7 and Day 21 (Figure 7A). Interestingly, only a thin layer (33 ± 13 μm) of tightly packed collagen was observed Day 21 (Figure 7B). Similar to the control, rapid material degradation was also observed for modified Bovine Pericardium by Day 7 in Figure 7A. A significant increase was observed in cell infiltration relative to the control (3712 ± 1724 cells/mm^2), with female grafts displaying a 3-fold increase in cells/mm^2 than male grafts. This value was found to be lowered considerably by Day 21 at 1409 ± 698 cells/mm^2 with less of a difference in response between male and female rats at this time (Figure 6B and 6C). Collagen deposited by the host was found in Day 21 samples and a measured thickness of 61 ± 8 μm is shown in Figure 7B. This difference is significant, a 2-fold increase in the thickness compared to the control samples.

Bovine dermis scaffolds showed delayed cell infiltration in the center with the majority of cells found at the host-material interface with only 748 ± 436 cells/mm^2 at day 7; this was true

for grafts placed in male and female rats. By Day 21, intact biomaterial was still seen with some cell presence in the material itself; although, this was not seen evenly throughout the material (Figure 6A). This qualitative observation was confirmed quantitatively with 1644 ± 1221 cells/mm^2 found for unmodified bovine dermis in Day 21 samples (Figure 6C). Measurements made from female samples were once again 3-fold higher than male values. Masson's Trichrome staining of unmodified bovine dermis samples showed little degradation at Day 7 and Day 21 (Figure 7A). Collagen fibrils were found at the muscle interface where the highest cell presence was seen on Day 7; by Day 21, these fibrils appeared to be more densely packed. Measurements of the collagen layer thickness determined the thickness of collagen layer to be 55 ± 21 μm on Day 21. High cell recruitment to the biomaterial edges was also seen for C18-modified bovine dermis. In this case, cell infiltration was calculated to be significantly higher in the modified dECM compared to the control for both time points studied and maintained over time (3184 ± 1314 cells/mm^2 at Day 7 and 3448 ± 1604 cells/mm^2 at Day 21). Aliphatic chain modification was apparent at the surfaces of modified bovine dermis samples on Day 7, as was the mainly intact dECM scaffold. Collagen found at the biomaterial edge was similar in structure to control samples. Some progression in biomaterial remodelling was observed in Day 21 samples, although much of the scaffold remained. The collagen layer deposited at the edge of C18-modified bovine dermis was more densely packed by Day 21, even to a greater extent than control scaffolds with collagen thickness measured to be 28 ± 5 μm (Figure 7B), half the thickness of control samples.

Variable cell infiltration was observed at the scaffold center of unmodified human dermis by Day 7 (1643 ± 1451 cells/mm^2). No cells were found at the center of grafts implanted in females (as shown qualitatively Figure 6A) while a considerable presence was detected in male

samples, noted in Figure 6B. Cell presence is maintained with 1153 ± 590 cells/mm^2 found at Day 21. Female and male response was found to be similar at the later time point (Figure 6C). The unmodified human dermis scaffold appeared largely intact by Day 7 and no vessel formation was observed. By Day 21, progressed material degradation and some early vascularization could be seen and the thickness of deposited collagen layer was 57± 15 μm; increased density of the deposited collagen layer between Day 7 and Day21 was evident qualitatively (Figure 7A). Again, modified samples elicit large accumulation of cells at the interface but reduced cell presence at the center (964 ± 1071 cells/mm^2 for modified human dermis at Day 7). By Day 21, material degradation had progressed, allowing for a higher cell presence in modified human dermis scaffolds (1704 ± 428 cells/mm^2). The characteristic bright red staining of C18 aliphatic chain presence was seen in stained Day 7 samples with the modified human dermis sample largely intact. Wavy fibrils of collagen different from the organization of collagen in the graft was observed. The thickness of collagen deposition at the interface by Day 21 had increased compared to control samples to 96 ± 37 μm (Figure 7B). Biomaterial degradation and vascularization were also delayed as more of the dECM was present relative to unmodified human dermis.

H+E and Trichrome staining showed that cell infiltration and biomaterial degradation was delayed *in vivo* for all tissue sources upon C18 modification at early time points, as suggested by earlier *in vitro* experiments. Cell-matrix interactions, including material remodelling and vascularization, was observed by Day 21 for both unmodified and modified scaffolds. The addition of hydrophobes did not appear to cause excess collagen deposition at the muscle-material interface for SIS or UBM samples but did cause a significant increase for pericardium

and human dermis samples. Bovine dermis samples showed an overall reduction in collagen deposition upon modification, indicating that the effect may vary with tissue source. There was no evidence of graft rejection in the form of excess fibrosis or the formation of foreign body giant cells in any of the scaffolds tested.

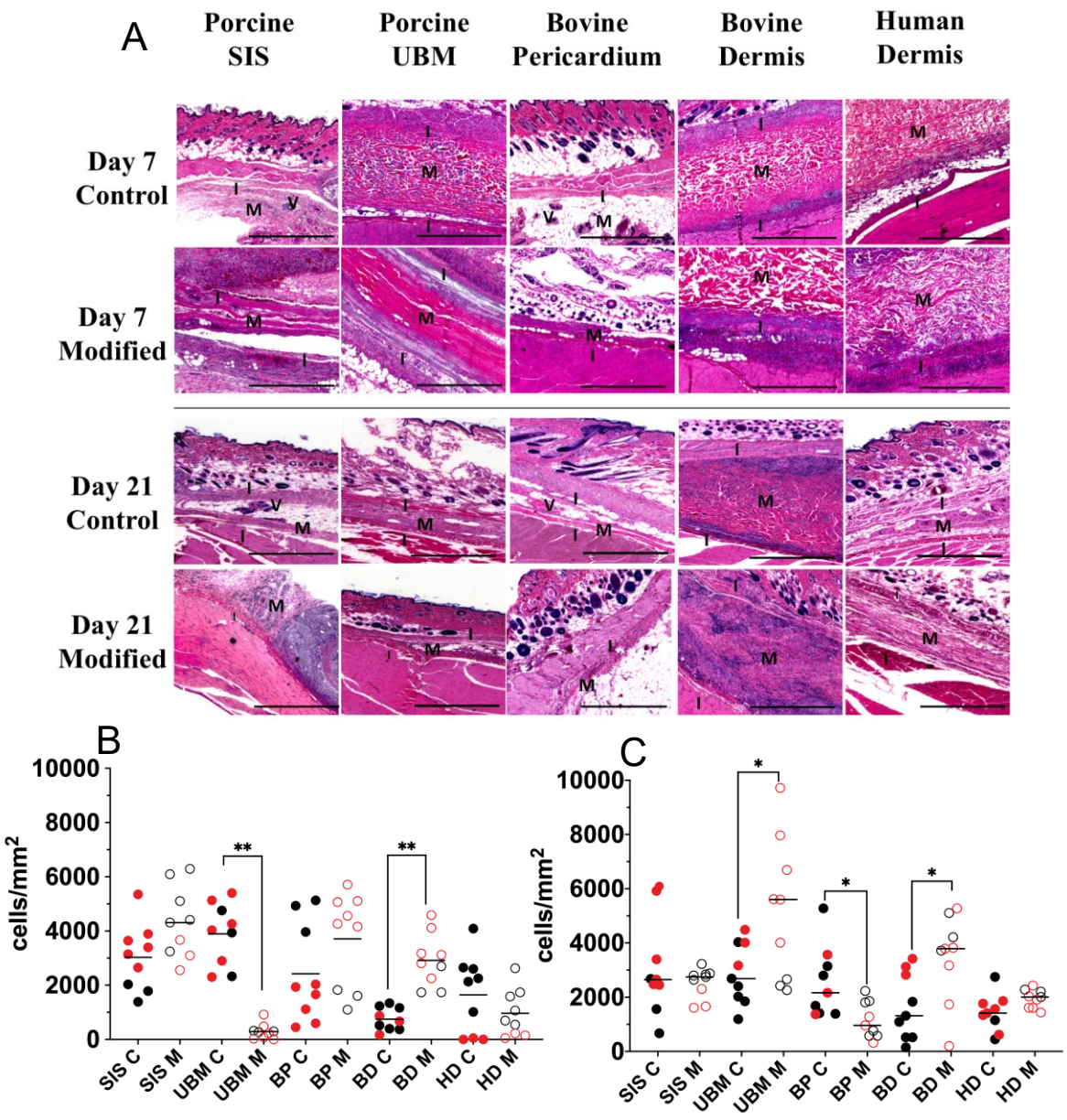

Figure 6. ***In vivo*** **subcutaneous biocompatibility of C18-modified dECM scaffolds through cell-material interactions: A)** H&E staining showed that cell infiltration to the center of dECM is delayed at Day 7 for modified scaffolds relative to control counterparts, cells present in center by day 21. Scale bar = 1000 μm I=Interface M=Material V=Vasculature. **B)** Quantification of cells present in the center of dECM at day 7 confirmed reduced cell infiltration for modified grafts (o) compared to control (•), but this largely varied between male (black) and female rats (red). **C)** Quantification of cells present in the graft center at day 21 confirms larger presence of cells at later time points in modified grafts (o) compared to control (•); again, response varied between male (black) and female rats (red).

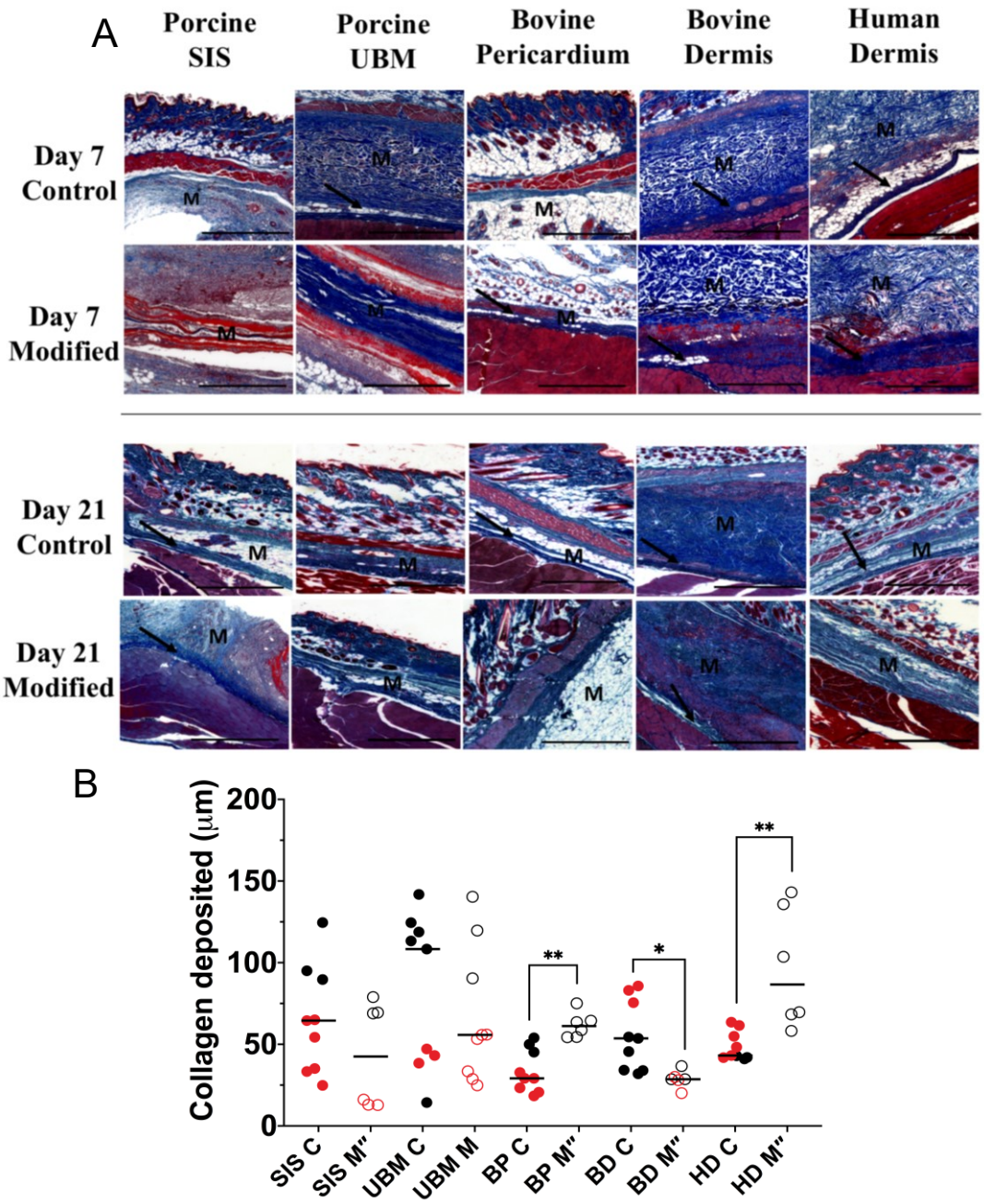

Figure 7. *In vivo* subcutaneous biocompatibility of C18-modified dECM scaffolds through collagen deposition: A) Trichrome staining showed collagen presence of dECM grafts at Day 7 and Day 21, as well as collagen deposited at graft-muscle interface (arrows) indicated by difference in organization Scale bar = 1000 μm M= Material. **B)** Quantification of collagen deposited at the muscle interface at day 21 showed differences in thickness for modified grafts (o) compared to control (•); response varied between male (black) and female rats (red). " denotes groups in which only two biological replicates were harvested.

4 Discussion

Decellularized extracellular matrices have long since been established as attractive biomaterials for tissue regeneration due to their inherent biocompatibility; both xenogeneic and allogenic sources have been shown to integrate into the host environment with reduced immune complications and dECM composition naturally includes important bioactive cues to promote cell-scaffold interactions[19]. The C18-modified dECMs presented here address the mechanical shortcomings observed in preclinical studies using dECM for bladder tissue regeneration by improving material extensibility to better mimic native bladder tissue (Figure 1). Although several researchers have endeavoured to improve outcomes using chemically modified dECMs, this is the first attempt to improve various decellularized scaffolds' ability to meet the bladder's load-bearing requirements. In the present work, we modified porcine SIS, porcine UBM, bovine pericardium, bovine dermis and human dermis by incorporating hydrophobes that act as transient crosslinkers to improve the viscoelastic dissipation at a molecular level and generate scaffolds of high toughness and compliance, in a manner similar to synthetic polymer and collagen scaffolds[27,30] .

The degree of modification, and as a result the mechanical properties, could be manipulated by reaction time (Figure 1). Soft tissues typically exhibit viscoelastic behavior[1] and we found that the addition of hydrophobes maintained this profile. Noncovalent interactions with aliphatic chains may result in conformational changes in the proteins present in dECMs; we exposed unmodified dECMs to a denaturing temperature (65^{o}C) in order to compare the partially denatured dECM to the unmodified and C18 modified samples. Porcine SIS, porcine UBM and

bovine pericardium are scaffolds of particular interest in reconstructive urology. Upon modification, all three dECMs exhibited increased compliance, as seen through the increased peak strain at a reduced peak stress relative to unmodified samples and elastic moduli closer to bladder tissue values (Table 1). Material toughness was not compromised but rather maintained or improved upon C18 addition for these materials. This is promising as it may extend the lifetime of these dECMs *in vivo* to act as support during the tissue regeneration process. Bovine dermis and human dermis samples also exhibited improvements in peak strain; however, peak stress, elastic moduli and toughness also all increased, indicating that aliphatic chain modification resulted in stiffer scaffolds for this tissue type (Table 1). Thermal denaturation also increased peak strain and reduced peak stress as well as elastic moduli; although, this was at the cost of drastically reduced material toughness values to those much lower than bladder tissue. Porcine SIS and human dermis are two exceptions to this observation, where peak stress and toughness were largely unaffected; this may be the result of the level of natural crosslinking present in these scaffolds.

Hydrophobe addition did not affect the dECM's ability to swell in an aqueous environment and allow for small molecule diffusion throughout the biomaterial, as the swelling profile and swelling ratio at 24 h were mostly unaffected by C18 modification at both reaction times (Figure 2 A-E). As previously mentioned, the noncovalent interactions between aliphatic chains and collagen fibrils may result in protein conformational changes. Any changes in the swelling profile that would be caused by the opening of the collagen triple helix to a random coil configuration is likely balanced out with the introduction of hydrophobes in the modified scaffolds. We attributed changes in the swelling ratio for porcine UBM modified with C18 for 1 h to a separation of the

laminated layers observed, and subsequent loss of material, after prolonged swelling at 37°C. Thermal denaturation had a larger effect on swelling, with increased swelling ratios seen most noticeably in porcine UBM, bovine pericardium and bovine dermis samples but not in porcine SIS or human dermis samples similar to the trend observed during tensile testing. This behavior further supports the use of hydrophobic groups as crosslinked junctions to improve mechanical properties as it does not affect the scaffolds' thermal stability in an aqueous environment.

C18 modification greatly improved resistance to enzymatic degradation for all dECM types compared to unmodified and thermally denatured dECMs (Figure 2 F-J). The protease degradation profile over time could be tunable by adjusting the reaction time as seen in Figure 2 G and Figure 2 H whereby a 2 h reaction time resulted in reduced material degradation over time compared to a 1 h reaction time for porcine UBM and bovine pericardium. In the case of UBM, the previously observed separation of laminated layers may have served to increase the surface area exposed to enzyme and cause more rapid degradation. These results further indicate the prolonged lifetime of the modified dECMs *in vivo*, addressing the secondary issue of rapid degradation of unmodified dECM scaffolds.

Surface hydrophobicity has been shown to affect protein adsorption on biomaterial surfaces, and by extension, the adhesion of surrounding cell types as well as their differentiation in the case of immune cells[34]. Definitive conclusions about cell adhesion and preference for hydrophilic vs. hydrophobic surfaces are conflicting and differ between cell types. A number of reports have found fibroblast adhesion and proliferation to be higher on hydrophilic surfaces[35–37] while opposing results have been reported for monocyte adhesion to hydrophobic surfaces[15,38]. Moreover, epithelialization has been seen to take several weeks on hydrophilic

porcine SIS[8], and corneal epithelial cell adhesion was not inhibited *in vitro* on hydrophobic surfaces[37].

Direct measurements of the surface contact angle confirmed that all dECM surfaces become more hydrophobic regardless of their initial affinity for water (Figure 3A). Fibroblasts showed much higher proliferation on control scaffolds, most noticeably on porcine SIS, bovine pericardium and bovine dermis, with the exception of human dermis (Figure 3B). All modified materials showed the ability to support cell adhesion; although, to a higher degree of variability. Delayed proliferation was observed with increased hydrophobicity, again with the exception of human dermis, that had minimal adhesion on both counts. Interestingly, macrophage adhesion was comparable between hydrophilic and hydrophobic surfaces (Figure 3C). While we observed a clear preference for hydrophilic surface for fibroblasts, this was not the case for bladder epithelial cells that preferred moderate hydrophobicity than either extremely hydrophilic surfaces or extremely hydrophobic surfaces. Delayed proliferation on modified materials further supports this observation. Unmodified bovine pericardium and bovine dermis were able to induce proliferation and epithelial cell performance was improved on human dermis samples over modified bovine dermis (Figure 3D). This suggests that extreme hydrophobicity may have a greater negative impact. Other properties of biomaterials such crosslinking degree, scaffold content and structure also play a role in cell migration and proliferation[39]. Since these factors varied across all dECMs and cell-material interactions are a result of a combination of these properties, future studies focused on characterizing cell behavior *in vitro* may include experimentation defining these properties in dECM in greater detail. Additionally, protein adsorption plays a strong role in cell adhesion and previous reports have shown that proteins

adsorb more on hydrophobic surface but also undergo a higher level of conformational change with increased surface hydrophobicity[35]. Proteins in complete media were allowed to adsorb onto dECM surface overnight; however, this may not be representative of the amount that may be adsorbed *in vivo* and cause difficulties in accurately evaluating material cytotoxicity *in vitro*.

Macrophages are considered one of the first responders to the implant site and interact with implanted materials[14,15]. Cytokine production by macrophages and other cells regulate the phenotypic response from other immune cells. Because of their role in implant rejection, macrophages are frequently implemented to evaluate the short-term immunomodulatory capacity of scaffolds *in vitro*. A shift towards an "M2" phenotype is desirable in biomaterial design to reduce inflammation at the implant site and signal the formation of new tissue to surrounding tissue-resident cells[40]. This is an especially important consideration in the urinary environment where there is a high exposure to toxins. While previous studies have found that dECM is resistant to bacterial infection[41], preclinical outcomes have reported inconsistent results due to graft contracture and inflammation from long-term exposure to urine[8,17,24]. We chose THP-1 monocytes to observe the response from human immune cells. We differentiated the monocytes into macrophages and exposed the cells to either stimulating cytokines or dECM scaffolds, control or modified, to observe differences in macrophage phenotype behavior. The delivery of signalling cytokines resulted in stronger upregulation in key surface marker expression (Figure 4) while exposure to a foreign biomaterial causes a shift in cytokine production (Figure 5). TNFα expression was substantially reduced in C18-modified dECM across all tissue sources, indicating a reduction in cytokine signalling for inflammatory immune cells (Figure 5). Increased TGFβ further indicated a shift towards a pro-regenerative phenotype. We observed changes in surface

marker expression towards an M2 phenotype to a lesser degree for most dECMs. We noticed a strong downregulation in the case of both unmodified and modified bovine and human dermis, indicating that these materials may not support macrophage differentiation *in vitro*. The incorporation of hydrophobes promoted CD68 and CD163 expression in modified bovine pericardium, the dECM that most strongly resembled rabbit bladder tissue in terms of mechanical properties. These results further support the use of C18 molecules to not only improve a scaffold's mechanical properties but also mitigate a pro-inflammatory response from macrophages. A reduced inflammatory reaction may also be beneficial in the potential use of cell-laden modified dECMs to reduce the potential for adaptive immune cells attacking foreign cells that would be present at the implant site.

The typical host response to a foreign body begins immediately upon implantation with protein adsorption, followed by immune cell infiltration and cytokine release over the course of the first week; subsequently, other cell types such as fibroblasts are recruited[42]. In the event that a biomaterial is not biocompatible (does not result in quick resolution of the initial inflammatory response), persistent infection and fibrous encapsulation is evident three to four weeks post-implantation[42,43].Changes in dECM composition can change the host's foreign body response. Therefore, we evaluated the impact of aliphatic chain modification on the host's behavior through subcutaneous implantation of unmodified and modified scaffolds by analysing cell infiltration, biomaterial degradation and collagen deposition at an early timepoint (Day 7) and later timepoint (Day 21). C18-modified materials showed delayed cell infiltration, except for modified bovine pericardium, with cells accumulating primarily at the interface on Day 7 (Figure 6); this dissipates by Day 21 as cells are able to penetrate to the biomaterial center. This

observation is expected as degradation of the biomaterial is known to activate the immune system response, which begins with cell accumulation at the site upon protease digestion and material remodelling[15,44]. We found a highly varied gender-based response at Day 7 in terms of cells present per unit area at the center of biomaterial (Figure 6). This becomes less obvious by Day 21 in modified materials, with the exception of modified UBM and unmodified bovine dermis.

Modified dECMs displayed reduced degradation compared to control *in vivo* when qualitatively evaluated through Masson's Trichrome staining (Figure 7) similar to the enzymatic degradation test performed with Collagenase I. The thickness of the newly deposited collagen layer was quantified for samples harvested on Day 21 to further study the host response. Collagen deposition varied not only between dECMs but also between control and modified samples. Porcine SIS, porcine UBM and bovine dermis all exhibited thinner layers of collagen at the interface upon modification while modified bovine pericardium and human dermis had significantly thicker layers compared to controls. A previous study conducted by Kyriakides et al. measured the thickness of collagen layers for subcutaneously implanted biomaterials and found encapsulated samples to have thickness greater than 150 μm[45]. It is noteworthy that no modified scaffold in this study had a reported thickness above 100 μm. Although biomaterial degradation and cell infiltration were delayed, this did not appear to result in fibrotic capsule formation or graft rejection. Longer term studies may be required to see if fibrotic capsule formation is truly mitigated or simply delayed with the addition of hydrophobes.

In summary, studies on cell adhesion and immunomodulation with modified and unmodified dECMs suggest that C18-modified dECMs may be suitable candidates for urologic

tissue regeneration. The addition of transient crosslinkers provides material strength and improves compliance to make dECMs more suitable for load-bearing applications. Further *in vivo* studies in the urodynamic environment, where dynamic loading and toxin presence may have an effect on macrophage polarization[42], cell infiltration and fibrosis formation would provide further clarity. Future directions may also include the addition of pre-adsorbed extracellular matrix molecules on C18-modified dECMs, thus combining mechanical properties mimicking native bladder tissue and protease resistance with improved cellular adhesion to further promote tissue regeneration.

5 Conclusions

The work presented here outlines a simple methodology for the incorporation of aliphatic chains in decellularized extracellular matrices to improve their mechanical properties such that they are better suited for bladder tissue engineering. The addition of hydrophobes did improve material compliance to more closely mimic native bladder tissue and improve protease resistance without negatively impacting material swelling in physiological conditions. The inherent bioactive cues in dECM offer a 3D microenvironment that supports cell adhesion; increased hydrophobicity through C18 modification did result in delayed proliferation for primary bladder fibroblasts and epithelial cells *in vitro*, but cell infiltration was supported *in vivo*. Modified dECMs, most noticeably bovine pericardium, also displayed immunomodulatory capacity *in vitro* with localized macrophage polarization towards a pro-regenerative M2 phenotype, which may improve preclinical outcomes for dECMs in a urodynamic environment. These promising results establish aliphatic chain modification as a viable strategy that tackles previous shortcomings of dECMs for the regeneration of biomechanically functional urinary tissues.

6 References

1. Ajalloueian, F., Lemon, G., Hilborn, J., Chronakis, I. S. & Fossum, M. Bladder biomechanics and the use of scaffolds for regenerative medicine in the urinary bladder. *Nat. Rev. Urol.* **15**, 155–174 (2018).
2. Chua, M. E., Farhat, W. A., Ming, J. M. & McCammon, K. A. Review of clinical experience on biomaterials and tissue engineering of urinary bladder. *World J. Urol.* (2019). doi:10.1007/s00345-019-02833-4
3. Lin, H.-K. *et al.* Understanding roles of porcine small intestinal submucosa in urinary bladder regeneration: identification of variable regenerative characteristics of small intestinal submucosa. *Tissue Eng. Part B. Rev.* **20**, 73–83 (2014).
4. Pokrywczynska, M., Gubanska, I., Drewa, G. & Drewa, T. Application of bladder acellular matrix in urinary bladder regeneration: the state of the art and future directions. *Biomed Res. Int.* **2015**, 613439 (2015).
5. Song, L. *et al.* Bladder acellular matrix and its application in bladder augmentation. *Tissue Eng. Part B. Rev.* **20**, 163–72 (2014).
6. Caione, P., Boldrini, R., Salerno, A. & Nappo, S. G. Bladder augmentation using acellular collagen biomatrix: a pilot experience in exstrophic patients. *Pediatr. Surg. Int.* **28**, 421–8 (2012).
7. Hosseini, J., Hosseini, S., Hosseini, M. A. & Rezaei, Y. Pericardium in Reconstructive Urologic Surgeries: A Systematic Review and Meta-Analysis. *Urol. Int.* **102**, 131–144 (2019).
8. Kundu, A. K., Gelman, J. & Tyson, D. R. Composite thin film and electrospun biomaterials for urologic tissue reconstruction. *Biotechnol. Bioeng.* **108**, 207–15 (2011).
9. Sadtler, K. *et al.* The Scaffold Immune Microenvironment: Biomaterial-Mediated Immune Polarization in Traumatic and Nontraumatic Applications. *Tissue Eng. Part A* **23**, 1044–1053 (2017).
10. Ashley, R. A. *et al.* Leukocyte inflammatory response in a rat urinary bladder regeneration model using porcine small intestinal submucosa scaffold. *Tissue Eng. Part A* **15**, 3241–6 (2009).
11. Brown, B. N. *et al.* Macrophage phenotype as a predictor of constructive remodeling following the implantation of biologically derived surgical mesh materials. *Acta Biomater.* **8**, 978–87 (2012).
12. Brown, B. N., Valentin, J. E., Stewart-Akers, A. M., McCabe, G. P. & Badylak, S. F. Macrophage phenotype and remodeling outcomes in response to biologic scaffolds with and without a cellular component. *Biomaterials* **30**, 1482–91 (2009).
13. Wissing, T. B. *et al.* Macrophage-Driven Biomaterial Degradation Depends on Scaffold Microarchitecture. *Front. Bioeng. Biotechnol.* **7**, 87 (2019).
14. Sridharan, R., Cameron, A. R., Kelly, D. J., Kearney, C. J. & O'Brien, F. J. Biomaterial based modulation of macrophage polarization: A review and suggested design principles. *Materials Today* (2015). doi:10.1016/j.mattod.2015.01.019
15. Mariani, E., Lisignoli, G., Borzì, R. M. & Pulsatelli, L. Biomaterials: Foreign Bodies or Tuners for the Immune Response? *Int. J. Mol. Sci.* **20**, (2019).

16. Sadtler, K. *et al.* Proteomic composition and immunomodulatory properties of urinary bladder matrix scaffolds in homeostasis and injury. *Semin. Immunol.* **29**, 14–23 (2017).
17. Davis, N. F. *et al.* Porcine extracellular matrix scaffolds in reconstructive urology: An ex vivo comparative study of their biomechanical properties. *J. Mech. Behav. Biomed. Mater.* **4**, 375–82 (2011).
18. Davis, N. F., Coakley, D. N., Callanan, A., Flood, H. D. & McGloughlin, T. M. Evaluation of xenogenic extracellular matrices as adjuvant scaffolds for the treatment of stress urinary incontinence. *Int. Urogynecol. J.* **24**, 2105–10 (2013).
19. Aamodt, J. M. & Grainger, D. W. Extracellular matrix-based biomaterial scaffolds and the host response. *Biomaterials* **86**, 68–82 (2016).
20. Boersema, G. S. A., Grotenhuis, N., Bayon, Y., Lange, J. F. & Bastiaansen-Jenniskens, Y. M. The Effect of Biomaterials Used for Tissue Regeneration Purposes on Polarization of Macrophages. *Biores. Open Access* **5**, 6–14 (2016).
21. Badylak, S. F. & Gilbert, T. W. Immune response to biologic scaffold materials. *Semin. Immunol.* **20**, 109–16 (2008).
22. Ge, L. *et al.* Preparation of laminin/nidogen adsorbed urinary bladder decellularized materials via a mussel-inspired polydopamine coating for pelvic reconstruction. *Am. J. Transl. Res.* **9**, 5289–5298 (2017).
23. Roth, C. C. *et al.* Bladder regeneration in a canine model using hyaluronic acid-poly(lactic-co-glycolic-acid) nanoparticle modified porcine small intestinal submucosa. *BJU Int.* **108**, 148–55 (2011).
24. Xiong, Q. *et al.* A nanomedicine approach to effectively inhibit contracture during bladder acellular matrix allograft-induced bladder regeneration by sustained delivery of vascular endothelial growth factor. *Tissue Eng. Part A* **21**, 45–52 (2015).
25. Gulyuz, U. & Okay, O. Self-Healing Poly(acrylic acid) Hydrogels with Shape Memory Behavior of High Mechanical Strength. *Macromolecules* **47**, 6889–6899 (2014).
26. Abdurrahmanoglu, S., Can, V. & Okay, O. Design of high-toughness polyacrylamide hydrogels by hydrophobic modification. *Polymer (Guildf).* **50**, 5449–5455 (2009).
27. Geng, Y. *et al.* Hydrophobic association mediated physical hydrogels with high strength and healing ability. *Polymer (Guildf).* **100**, 60–68 (2016).
28. Bilici, C. & Okay, O. Shape Memory Hydrogels via Micellar Copolymerization of Acrylic Acid and n -Octadecyl Acrylate in Aqueous Media. *Macromolecules* **46**, 3125–3131 (2013).
29. Carignan, D., Désy, O., Ghani, K., Caruso, M. & de Campos-Lima, P. O. The size of the unbranched aliphatic chain determines the immunomodulatory potency of short and long chain n-alkanols. *J. Biol. Chem.* **288**, 24948–55 (2013).
30. Yu, C. *et al.* Aliphatic Chain Modification of Collagen Type I: Development of Elastomeric, Compliant, and Suturable Scaffolds. *ACS Appl. Bio Mater.* **3**, 1331–1343 (2020).
31. Zarif, J. C. *et al.* A phased strategy to differentiate human CD14+monocytes into classically and alternatively activated macrophages and dendritic cells. *Biotechniques* **61**, 33–41 (2016).
32. Menzies, K. L. & Jones, L. The Impact of Contact Angle on the Biocompatibility of Biomaterials. *Optom. Vis. Sci.* 1 (2010). doi:10.1097/OPX.0b013e3181da863e
33. Kim, S., Layton, C. & Bancroft, J. D. *Bancroft's theory and practice of histological*

techniques. (Elsevier, 2019).
34. Wang, Y.-X., Robertson, J. L., Spillman, W. B. & Claus, R. O. Effects of the chemical structure and the surface properties of polymeric biomaterials on their biocompatibility. *Pharm. Res.* **21**, 1362–73 (2004).
35. Anselme, K., Ploux, L. & Ponche, A. Cell/Material Interfaces: Influence of Surface Chemistry and Surface Topography on Cell Adhesion. *J. Adhes. Sci. Technol.* **24**, 831–852 (2010).
36. Lee, J. H., Lee, S. J., Khang, G. & Lee, H. B. Interaction of fibroblasts on polycarbonate membrane surfaces with different micropore sizes and hydrophilicity. *J. Biomater. Sci. Polym. Ed.* **10**, 283–94 (1999).
37. Schweikl, H. *et al.* Proliferation of osteoblasts and fibroblasts on model surfaces of varying roughness and surface chemistry. *J. Mater. Sci. Mater. Med.* **18**, 1895–905 (2007).
38. Boehler, R. M., Graham, J. G. & Shea, L. D. Tissue engineering tools for modulation of the immune response. *Biotechniques* **51**, 239–40, 242, 244 passim (2011).
39. Dziki, J. L., Huleihel, L., Scarritt, M. E. & Badylak, S. F. Extracellular Matrix Bioscaffolds as Immunomodulatory Biomaterials. *Tissue Eng. Part A* **23**, 1152–1159 (2017).
40. Schutte, R. J., Parisi-Amon, A. & Reichert, W. M. Cytokine profiling using monocytes/macrophages cultured on common biomaterials with a range of surface chemistries. *J. Biomed. Mater. Res. A* **88**, 128–39 (2009).
41. Davis, N. F., McGuire, B. B., Callanan, A., Flood, H. D. & McGloughlin, T. M. Xenogenic extracellular matrices as potential biomaterials for interposition grafting in urological surgery. *J. Urol.* **184**, 2246–53 (2010).
42. Sridharan, R., Cameron, A. R., Kelly, D. J., Kearney, C. J. & O'Brien, F. J. Biomaterial based modulation of macrophage polarization: a review and suggested design principles. *Mater. Today* **18**, 313–325 (2015).
43. Anderson, J. M., Rodriguez, A. & Chang, D. T. Foreign body reaction to biomaterials. *Semin. Immunol.* **20**, 86–100 (2008).
44. Luttikhuizen, D. T., Harmsen, M. C. & Luyn, M. J. A. Van. Cellular and Molecular Dynamics in the Foreign Body Reaction. *Tissue Eng.* **12**, 1955–1970 (2006).
45. Kyriakides, T. R. *et al.* The CC chemokine ligand, CCL2/MCP1, participates in macrophage fusion and foreign body giant cell formation. *Am. J. Pathol.* **165**, 2157–66 (2004).

Curriculum Vitae

Sarah Rajani

727 West 40th Street, Baltimore, MD, 21211

Phone: 415.619.0693 Email: sarah.rajani@hotmail.com

PROFESSIONAL GOALS:

I am passionate about the safe and efficient development of novel cellular therapeutics for the treatment of severely debilitating diseases such that they are accessible for all patients who require them. My goal is to pursue a career in process development, researching new methods to produce therapeutic products or tackling problems surrounding scale-up of such processes. I believe in the importance multidisciplinary teams to better understand mechanisms and improve treatment outcomes.

EDUCATION:

Johns Hopkins University **Baltimore, MD**
Master of Science, Biomedical Engineering May 2020

Relevant Courses: Tissue Engineering, Cell Engineering, Engineering Principles of Drug Delivery, Systems Pharmacology and Population Pharmacokinetics, Advanced Topics in Regenerative and Immune Engineering, Physical Chemistry of Macromolecules

University of British Columbia **Vancouver, Canada**
Bachelor of Applied Science, Chemical and Bioprocess Engineering May 2018

Relevant Courses: Bioprocess Engineering I + II, Kinetics and Reactor Design, Process Dynamics and Control, Fundamentals of Cell Biology, Introductory Medical Biochemistry, Thermodynamics, Transport Phenomena I + II, Biological Process and Product Design

EXPERIENCE:

Brady Urological Institute - Johns Hopkins University **Baltimore, MD**
Graduate Researcher 2019-Present

- Performs DOE, data collection and analysis for the evaluation of newly developed biomaterials for bladder tissue regeneration
- Develops experimental protocol to investigate immune response *in vitro* and *in vivo*
- Compiles statistically significant data in written report and oral presentation format

Orthopaedics Research – St. Paul's Hospital **Vancouver, Canada**
Clinical Research Assistant 2017

- Performed study procedures as per Research Ethics Board guidelines
- Retrospectively reviewed medical records for 800 participants as part of data clean-up efforts
- Compiled available study data in datasets for statistical analysis for Private Investigators, fellows and medical students

Michael Smith Laboratories – University of British Columbia **Vancouver, Canada**
Undergraduate Researcher 2015

- Optimized morphology and size distributions of alginate macrocapsules
- Tested glass siliconization protocols to improve process reproducibility
- Studied the use of density gradient centrifugation for product purification

Skills:

Languages: Fully fluent in written and oral French, intermediate conversation level Urdu

UV Spectroscopy, CD Spectroscopy, NMR, Primary Cell Culture, In vitro macrophage studies, RT-qPCR, Biomechanics, Histochemical Staining, Bioreactor Design, Programming (MATLAB, R), Design of Experiments, Clinical Research Management, Pharmacokinetic modelling, Microsoft Office and Access